Assessing the impact of prereduction parameters on Mn ore from the Kalahari Manganese Field

by B.M.V. Baloyi, D. Chetty, D. Mchabe

Affiliation:
Mintek, Randburg, South Africa

Correspondence to:
B.M.V. Baloyi

Email:
BebertoB@mintek.co.za

Dates:
Received: 25 Oct. 2024
Published: March 2025

How to cite:
Baloyi, B.M.V., Chetty, D., Mchabe, D. 2025. Assessing the impact of prereduction parameters on Mn ore from the Kalahari Manganese Field. *Journal of the Southern African Institute of Mining and Metallurgy*, vol. 125, no. 3, pp. 121–128

DOI ID:
https://doi.org/10.17159/2411-9717/770/2025

ORCiD:
B.M.V. Baloyi
http://orcid.org/0000-0003-1332-8374
D. Chetty
http://orcid.org/0000-0002-1913-7598
D. Mchabe
http://orcid.org/0000-0002-9422-6750

This paper is based on a presentation given at the Mintek@90 Conference 2024, 11-12 November 2024, Sandton Convention Centre, Johannesburg, South Africa

Abstract

South Africa accounts for the largest global manganese ore production share, primarily from its Kalahari Manganese Field deposit. Despite this, domestic smelting is beset by energy constraints, resulting in most ore being exported for smelting. Mintek is investigating energy-efficient pathways for ore reduction, specifically undertaking prereduction tests to reduce energy consumption for manganese smelting. The present contribution considers the effect of methane, anthracite, and holding time, at a fixed temperature, on the extent of reduction of Mamatwan-type ore, primarily from a mineralogical perspective. In particular, the aim was to carburise the monoxide Mn phase to Mn carbide, as this is less energy intensive than producing metallic Mn from the monoxide. Based on thermogravimetric test results, the ore and products from three experiment sets were analysed using X-ray diffraction and scanning electron microscopy to assess the phases and textures present. The findings show that carburisation of manganese monoxide and its equivalents is most advanced under conditions of 8% anthracite, 10% methane, and 60 minutes of holding time, thus confirming with the thermogravimetric data. These results show promise for reducing energy consumption for Mn smelting in ferromanganese production.

Keywords

manganese, prereduction, mineralogical characterisation and low energy

Introduction

Manganese is an important metal used in a wide range of industries (battery, steel, electronics, and alloys). South Africa, with its world-class manganese resources, is a significant contributor to the global production of manganese. The country's large manganese mine operations over the recent years have further solidified its position in the industry. While most of the manganese produced globally is sourced from South Africa, most of this ore is exported to other countries for beneficiation. The remainder of the ore not exported is used to feed the local smelters. South Africa also has the potential to become a major player in the smelting space, but key data show that there are issues that have delayed the initiative to expand this industry. For example, the data show that South Africa has reduced its smelting capacity, where previously, 50% of the ore produced was smelted locally compared to only 16% of the ore smelted locally, as recorded in 2014 (Steenkamp et al., 2018). The decrease in the amount of ore processed locally is also linked to the increased mine production over the years, whereas the expansion of local smelting industries did not keep up to accommodate the increased mine production. The non-growth of this industry was mostly due to the instabilities in global manganese prices, energy costs, and availability. Over the years, these issues affected the industry, leading to the closure of some operations and, in some cases, resulted in job losses. In addition to that, the power utility company in the country has been struggling to meet the demand, which is projected to increase over the coming years. This is because of the projected increase in the population and the creation of new industries to power up the economy. As stated, a considerable amount of energy is required to produce manganese alloys, which comes with high cost implications. South Africa is currently facing energy issues related to the continuous increase in electricity tariffs and the unavailability of energy. In addition, the increased carbon taxes and environmental impact issues have contributed to a reduction in domestic smelting capacity. Finding new ways, or improving existing processes, to recover ferromanganese and silicon manganese alloys is much needed. A research project at Mintek aims to contribute to finding efficient ways to achieve higher recoveries of ferromanganese and manganese alloys from prereduced manganese using a CH_4-H_2-Ar gas mixture while lowering energy consumption. The present contribution focuses on the mineralogy of a selected low-grade ore from the Kalahari Manganese Field (KMF), aiming to understand the effect

of different parameters (temperature, holding time, and methane concentration) during its prereduction on various products derived from a series of tests.

Geology and mineralogy of ores of the Kalahari Manganese Field, South Africa

The Kalahari Manganese Field (KMF) in South Africa, is a giant ore body that accounts for ~75% of the world's land-based manganese ore resources. This region alone produces most of the mined Mn ore globally, at ~38% annually, compared to other countries (USGS, 2024). The Mn ore is hosted within the Hotazel Formation, occurring in three distinct layers interbedded with banded iron formation and hematite lutite layers. The KMF is characterised by three ore types based on their mineral assemblages and associated alteration styles. The Wessels ore type is high-grade (> 45% Mn), predominantly made up of Mn oxides, and represents a hydrothermally altered ore. The Mamatwan ore type is a low grade ore of Mn at ~38% and appears to be the least altered ore type, comprising Mn oxide and carbonate mineral assemblages. Intermediate characteristics of the Wessels and Mamatwan ore types characterise the supergene ore type. This ore has a variable Mn grade of 38% to 45% and is rich in both Mn-bearing carbonates and oxides, as well as containing oxyhydroxides typical of supergene ore. The Mamatwan type represents the largest portion of the resource, at ~97%, followed by the Wessels type at ~3%, and Supergene type at ~1%. Geographically, the Mamatwan type occurs throughout the ore body, whereas the Wessels type is restricted to the northern part of the deposit, and the Supergene type occurs along the eastern and northern sub-outcrops of the KMF. The Mn carbonate assemblages include kutnohorite, $Ca(Mn,Mg)(CO_3)_2$, Mn-calcite, $(Ca,Mn)CO_3$, and Mn oxide phases include hausmannite, $Mn^{2+}Mn_2^{3+}O_4$, bixbyite, $(Mn,Fe)_2O_3$, and braunite II, $Ca(Mn^{3+}Fe^{3+})_{14}SiO_{24}$. The supergene phases include manganomelane, $KMn^{4+}{}_7Mn^{3+}O_{16}$, manganite, MnO(OH) and pyrolusite, MnO_2.

Prereduction of Mn ores

Pyrometallurgical processing of manganese ore is an energy-consuming activity. Over the past years, new processes have been introduced to curb the high energy consumption during this process. One of these new ways was to introduce a prereduction stage prior to the final stage of ore smelting. Considering that the reduction of stable oxides requires higher energy inputs, the prereduction of Mn ores using gas reductants such as CH_4-H_2-Ar gas mixtures allows for reduction to take place at relatively lower temperatures (Bhalla, 2018). The reduction of the Mn ore at lower temperatures translates to lower energy inputs. In addition, during the traditional smelting process, mineralogical data is not necessarily required; rather, elemental chemistry data is preferred for assessing the ore feedstock. This manner of operation does not consider the type of minerals that host Mn. Besides that, ore body variability is generally quite common due to different geological processes that take place, as is evident from the different ore types present in the KMF, as well as variability within specific ore types (e.g., Chetty, 2008). These processes may result in the ore containing variable mineralogical compositions in terms of the Mn host mineral contributions to the grade. As such, the use of elemental chemistry data alone will not be able to account for the types of minerals present at any given geographical location of the ore body. The formation and decomposition of minerals is an energy-consuming activity; each mineral phase has unique requirements. Given that each mineral phase requires a variable amount of energy to decompose, it is thus necessary to understand the behaviour of mineral phases in the feed sample prior to processing. The typical reactions that may take place during the reduction stage, as presented by Reactions 1 to 10 (Wellbeloved et al., 1990; Tangstad et al., 2015; Chetty, Gutzmer, 2018) are provided in the following. Based on these reactions, the reduction of higher Mn oxides occurs exothermically as opposed to the endothermic reaction associated with the lower Mn oxides.

$$MnO_2 + {}^1/_4\,C = {}^1/_2\,Mn_2O_3 + {}^1/_4\,CO_2 \qquad \Delta H°298 = -56.8\ kJ \quad [1]$$

$${}^1/_2\,Mn_2O_3 + {}^1/_{12}\,C = {}^1/_3\,Mn_3O_4 + {}^1/_{12}\,CO_2 \qquad \Delta H°298 = -16.3\ kJ \quad [2]$$

$${}^1/_3\,Mn_3O_4 + {}^1/_6\,C = MnO + {}^1/_6\,CO_2 \qquad \Delta H°298 = +11.8\ kJ \quad [3]$$

$$MnO + C = Mn + CO \qquad \Delta H°298 = +274.5\ kJ \quad [4]$$

$$MnO_2 + {}^1/_2\,CO(g) = {}^1/_2\,Mn_2O_3 + {}^1/_2\,CO_2(g) \qquad \Delta H°298 = -99.9\ kJ \quad [5]$$

$${}^1/_2\,Mn_2O_3 + {}^1/_6\,CO(g) = {}^1/_3\,Mn_3O_4 + {}^1/_6\,CO_2(g) \qquad \Delta H°298 = 31.3\ kJ \quad [6]$$

$${}^1/_3\,Mn_3O_4 + {}^1/_3\,CO(g) = MnO + {}^1/_3\,CO_2(g) \qquad \Delta H°298 = -16.9\ kJ \quad [7]$$

$$MnO(l) + C = Mn(l) + CO(g) \qquad \Delta H°298 = +246.8\ kJ \quad [8]$$

The desirable carbothermic reduction reactions for higher Mn oxides in Reaction 1 to 8 show that their reduction is accompanied by the release of CO_2 at temperatures above 800 ^{0}C. Since the ore also consists of other phases such as carbonates, etc., the following Reactions 9 and 10 for calcite and dolomite may take place, respectively. Generally, the reactions are highly endothermic, and carbonate decomposition results in the release of CO_2.

$$CaCO_3 = CaO + CO_2(g) \qquad \Delta H°298 = +178.3\ kJ \quad [9]$$

$$CaMg(CO_3)_2 = CaO{\cdot}MgO + 2CO_2(g) \qquad \Delta H°298 = +295.4\ kJ \quad [10]$$

Reactions 1 to 10 represent the prereduction of higher manganese oxide and the decomposition of carbonates. These reactions take place in the prereduction zone. Reactions 11 to 15 represent the carburisation of MnO species using methane gas (Rankin, Van Deventer, 1980; Rankin, Wynnyckyj, 1997). These carburisation reactions take place at temperatures ranging from 1000^{0}C to 1300^{0}C (Kuo, Persson, 1954). The most likely carbide to be formed under these conditions is Mn_7C_3. However, Mn_5C_2 also forms, as given by Reaction 15.

$$7MnO + 3CH_4 + 8H_2 = Mn_7C_3 + 14H_2O \quad [11]$$

$$7MnO + 10CH_4 = Mn_7C_3 + 7CO + 20H_2 \quad [12]$$

$$CH_4 = C + H_2 \quad [13]$$

$$7MnO + 10C = Mn_7C_3 + 7CO \quad [14]$$

$$5MnO + 9CO = Mn_5C_2 + 7CO_2 \quad [15]$$

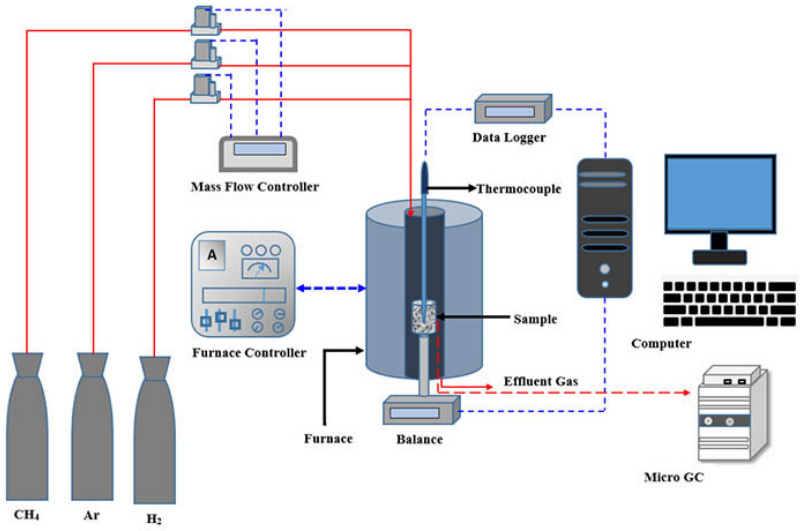

Figure 1—Schematic representation of experimental set-up for thermogravimetric analyses

Methodology

Raw material

Low-grade, Mamatwan-type manganese ore from the KMF, anthracite, and organic binder (Alcotac@ CB6), which is a copolymer of acrylic acid and acrylamide (from BASF, South Africa), were subjected to pelletisation. Before pelletising, the respective raw materials were characterised with regard to proximate analysis (anthracite – using the ASD-MET-C16/26 method) and chemical analyses (manganese ore – using the Mintek internal methods of ICP FEMN and XRF Q SCAN).

Thermogravimetric analysis

A series of thermogravimetric experiments to measure the mass loss during the prereduction of manganese composite pellets was conducted in a top loading thermogravimetric analyser housed in Mintek's Pyrometallurgy Division Laboratories. The schematic representation of the experimental setup can be seen in Figure 1, where the vertical type resistance furnace is connected to a proportional-integral-derivative (PID) controller. The temperature of the hot zone was maintained at ± 5 °C.

A continuous flow of argon gas at a rate of 1 L/min was introduced into the furnace to control the atmosphere. Pellet samples (5 g–15 g) were placed in a basket positioned retort fixed on a balance with high accuracy (0.1 mg). The data logging computer recorded the mass changes of samples. The temperature was ramped to a desired temperature (1000°C, 1200°C, or 1300°C) at a rate of 10°C/min, where it was kept constant. At a set temperature, the reaction gas (consisting of 5–10 vol % CH_4, 50 vol % H_2, and balance Ar) was introduced and allowed to flow at a set flow rate (2 L/min) until no mass change was observed.

After the prereduction experiment, the prereduced pellets were cooled to room temperature in an inert argon environment (i.e., the TGA was flushed with argon flowing at 1 L/min until room temperature was attained). The processes that are considered to take place are moisture removal, devolatilisation of anthracite, pyrolysis of the binder, pyrolysis of anthracite, reduction of manganese ore, and carburisation of oxides derived from manganese ore.

Mineralogical analysis

Mineralogical analysis was carried out on a total of 11 samples. Of those, one was the ore sample, sourced from the KMF, and the others were prereduced samples. The prereduced samples are made up of 3 batches representing product sets from different experimental conditions (Table 1). Two representative portions for all the samples were obtained post-splitting. The first portion was pulverised and subjected to qualitative XRD analysis for relative modal abundances, with quantitative mineral abundance determined on the ore sample only. This is because prereduced samples were expected to contain intermediate phases of poor or ill-defined structure. The other portions were prepared into a polished section and subjected to the SEM to obtain backscattered electron (BSE) images and energy dispersive spectrometry (EDS) analysis to track changes between the baseline ore sample and prereduced samples.

Table 1

Experimental set-up for the different parameters investigated with the controlled parameters

Parameters	Experiment Set 1	Experiment Set 2	Experiment Set 3
Temperature (°C)	1200	1200	1200
Anthracite (Vol.%)	0, 8, 12	8	8
Time (min)	60	60	30, 60, 90
Methane (Vol.%)	10	0, 2, 5, 10	10
Mass (g)	10	10	10

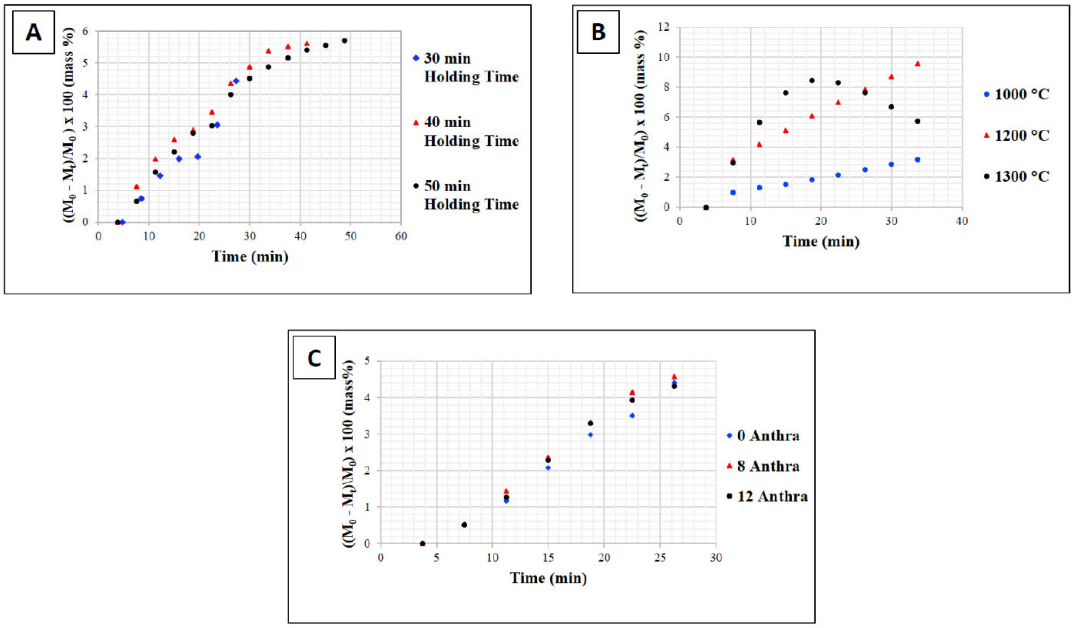

Figure 2—Thermogravimetric analyser results—Anthracite

Table 2
Bulk chemical composition of the ore sample

Oxide	Al_2O_3	CaO	Cr_2O_3	Fe_2O_3	MgO	MnO	SiO_2	CO_2
Wt%	<0.09	12.83	<0.07	7.92	4.22	47.6	6.61	16.71

Results and discussion

TGA results

The observed results from the TGA experiments are summarised in Figure 2. In the experiments to establish the optimum holding time, the weight-loss percentages were observed (Figure 2(a)) to reach a plateau at holding times of around 50 minutes. This observation informed that the tests in this study be carried out at a holding time of 60 minutes. This holding time agrees with the holding times of Anacleto et al. (2004), who reported that the formation of ferromanganese carbide was completed in 120, 60, and 45 min at 1000°C, 1100°C, and 1200°C, respectively. Despite the reduction being considered to increase with the increasing temperature (Ostrovski et al., 2004; Kononov et al., 2009), the temperature of 1200°C was observed to be optimum (Figure 2(b)). The decrease in the rate and extent of reduction on increasing the temperature to 1300°C can be associated with sintering and formation of semi-liquid silicate slags. Under the experimental conditions of this study, the effect of increasing anthracite content was observed to be insignificant. This observation is consistent with the results reported by Kononov et al. (2009) for carbon content ranging from 12 to 30 w/w%.

Ore characterisation

As observed in Tables 2 and 3, the ore sample has chemical and mineralogical concentrations consistent with a Mamatwan ore type. The major manganese-bearing minerals include braunite, hausmannite, and kutnohorite. Based on observations made from SEM, the sample can be set apart from the prereduced samples because of the well-preserved distinct textures observed (Figures 3A and B). Meanwhile, the prereduced samples display irregular textures. In the ore sample, the hausmannite phase appears to occur interstitially in a matrix of kutnohorite and serpentine. (Figure 3A). The SEM observations are aligned with the quantitative XRD analysis, which includes similar phases such as kutnohorite, hausmannite, calcite, and bixbyite (Figures 3A and B), identified in both techniques.

Mineralogical characterisation of the prereduced products

It is clear from the mineralogy of the prereduced samples that reduction has taken place. The extent to which reduction has

Table 3
Bulk mineralogy of the ore sample

Mineral	Ideal Chemical Formula	Mass%
Braunite	$Mn^{2+}Mn^{3+}{}_6SiO_{12}$	28.2
Bixbyite	$(Mn^{3+},Fe^{3+})_2O_3$	<1
Hausmannite	$Mn^{2+}Mn^{3+}{}_2O_4$	19.9
Kutnohorite	$Ca(Mn,Mg,Fe^{2+})(CO_3)_2$	23.6
Jacobsite	$(Mn^{2+},Fe^{2+},Mg)(Fe^{2+},Mn^{3+})_2O_4$	4.6
Calcite	$CaCO_3$	12.6
Hematite	Fe_2O_3	3.8
Serpentine	$Mg_3Si_2O_5(OH)_4$	6.3
Quartz	SiO_2	<1

Table 4

Qualitative relative phase proportions in four prereduced samples, investigating the effect of methane concentration on reduction extent

Compound Name	Ideal Formula	0% CH_4	2% CH_4	5% CH_4	10% CH_4
Manganosite	MnO	x	x	x	x
Iron manganese oxide	(Fe,Mn)O	xx	xx	xx	xx
Manganese magnesium oxide	(Mg,Mn)O	xx	x	xx	xx
Manganese carbide A	Mn_7C_3	xx	xxx	xxx	xxxx
Manganese carbide B	Mn_5C_2	xx	xx	xx	xx
Iron manganese	$Fe0.3Mn0.7$	x	x	x	x
Gehlenite	$Ca_2Al(AlSiO_7)$	xx	xx	xx	xx
Bredigite	$Ca_7Mg(SiO_4)_4$	xxx	xxx	xxx	xx
Kirschsteinite	$CaFe^{2+}SiO_4$	xx	xx	xx	xx
Graphite	C	xx	xx	xx	xx

Trace (< 5% wt.% x), minor (5-15 wt.% xx), intermediate (15-30 wt.% xxx), major (30-50 wt.% xxxx) and predominant (>50 wt.% xxxxx)

taken place is reflected by the presence of manganese oxides and manganese carbides in accordance with Reactions 1 to 8 and 11 to 15, respectively. The extent of reduction for samples investigating the effect of methane concentration on prereduction was confirmed through XRD analysis. The relative abundances of phases identified during reduction for the methane samples are given in Table 4. The 0% methane sample is primarily made up of bredigite, with gehlenite, manganese carbides, iron manganese oxide, and manganese magnesium oxide that range from minor to intermediate concentrations. Meanwhile, the 10% methane sample has a higher relative abundance of manganese carbides in major to minor proportions, with lower abundances of bredigite present. Based on these results, the concentration of methane does influence reduction extent, and this is shown by the variable relative abundances of reduction indicator phases such as manganese carbides (Mn_7C_3 and Mn_5C_2), iron manganese, and manganosite (MnO), with its solid solution equivalents manganese magnesium oxide and iron manganese oxide.

Table 5 presents the relative mineral abundances of the samples, investigating the effect of anthracite concentration on the prereduction of Mn ores. The XRD analysis reveals a relatively high presence of reduction indicator phases (as defined in the aforementioned). Similar to the trend reported for the methane samples, the relative abundances of phases present in the anthracite samples are variable with increasing abundances of anthracite. The 0% anthracite sample records a relatively lower combined abundance of the reduction indicator minerals as opposed to the relative higher abundance recorded in the 12% anthracite sample.

Table 5

Qualitative relative phase proportions in three pre-reduced samples investigating the effect of anthracite concentration on reduction extent

Compound Name	Ideal Formula	0 % Anthracite	8 % Anthracite	12 % Anthracite
Manganosite	MnO	x	x	x
Iron manganese oxide	(Fe,Mn)O	xx	xx	xx
Manganese magnesium oxide	(Mg,Mn)O	xx	xx	xxx
Manganese carbide A	Mn_7C_3	xxx	xxx	xxx
Manganese carbide B	Mn_5C_2	xx	xx	xx
Iron manganese	$Fe_{0.3}Mn0.7$	x	x	x
Gehlenite	$Ca_2Al(AlSiO_7)$	xx	x	x
Bredigite	$Ca_7Mg(SiO_4)_4$	xxx	xxx	xxx
Kirschsteinite	$CaFe^{2+}SiO_4$	xx	xx	xx
Graphite	C	-	x	-
Iron Silicon	$Fe_{11}Si_5$	-	-	x

Not detected (-), trace (< 5% wt.% x), minor (5-15 wt.% xx), intermediate (15-30 wt.% xxx), major (30-50 wt.% xxxx) and predominant (>50 wt.% xxxxx)

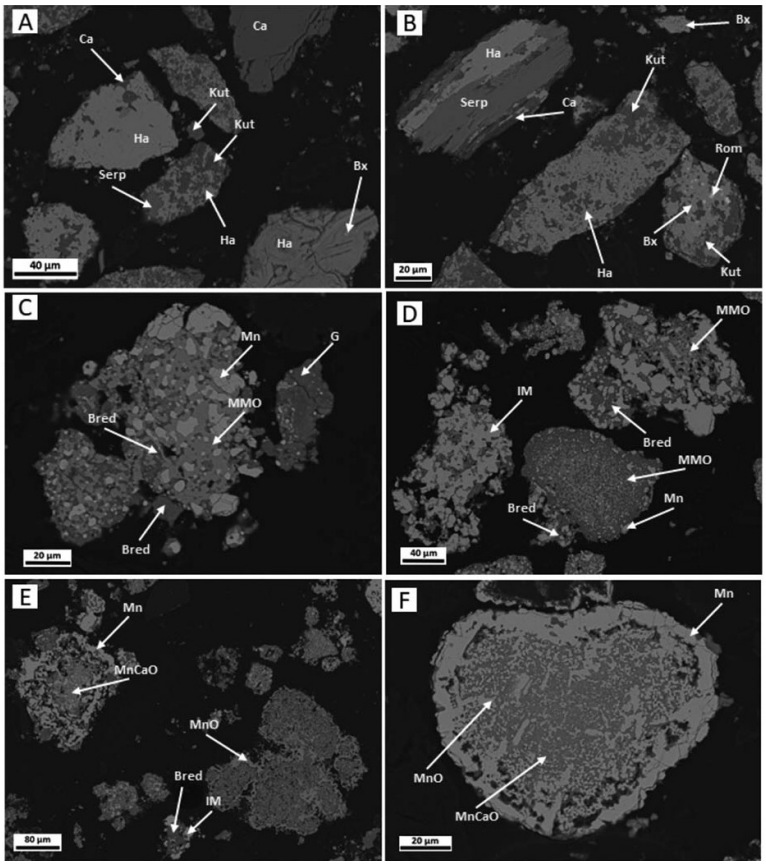

Figure 3—Backscattered electron images of the ore and prereduced samples under different conditions (A-F). (A-B) Ore sample with original textures. (C-D) Manganese carbides, manganese magnesium oxides, and iron-manganese with silicate phases for the methane and anthracite samples respectively, in an altered texture from that of the ore. (E-F) Reaction rims of manganese carbides and oxides with enclosed phases of manganese calcium oxides represent partially reduced particles. He – hematite, Br – braunite, Kut – kutnohorite, Ha – hausmannite, Ca – calcite, Bx – bixbyite, Rom – romanechite, Serp - serpentine, Mn – manganese carbide, MMO – manganese magnesium oxide, G – gehlenite, Bred - bredigite, IM – iron manganese, MnO – manganese oxide, and MnCaO – manganese calcium oxide phases

The vice versa applies to other of the phases present in the samples. Furthermore, the results reveal that the increase in anthracite concentrations corresponds with the formation of new phases. These phases are in the 8% anthracite sample where graphite is observed, and the 12% anthracite sample, in which the iron silicon phase is observed.

The relative phase abundances in the samples investigating the effect of holding time are presented in Table 6. The observations made are in line with the reduction reactions presented in this paper. The relative abundances of the reported phases are variable, and it is evident that reduction has occurred. The XRD analysis does not detect the presence of manganosite, magnesium manganese oxide, and iron manganese oxide in the 60- and 90-minutes samples, as opposed to the 20-minute sample where these phases were detected. Higher relative abundances of manganese carbides and iron manganese phases are recorded instead, which could suggest the additional time allowed for more extensive reduction to take place. As such, the absence of manganosite and its solid solution equivalents may be due to the carburisation process, as given by Reactions 11 to 15. Additionally, a slight decrease in the relative abundance of Mn_7C_3 is observed from the 60-minute to the 90-minute sample, possibly due to a change in environment. A change in environment over time may favour the formation of other phases in the sample, such as the increased relative abundances of iron manganese and other alloy phases.

Overall, the XRD analysis confirmed that reduction had taken place, and that the manganese ore was predominantly reduced to Mn_7C_3 and Mn_5C_2. The relative abundance of Mn_7C_3 was higher than that of Mn_5C_2 across all the prereduced samples analysed. Other species associated with reduction include iron manganese, manganese iron carbide, manganosite, and the solid solution equivalents of manganosite. The XRD highlights that the increase of methane gas and anthracite concentrations during reduction corresponds to optimal results through the formation of carbides. Finally, the extent of reduction of manganese oxides based on the results appears to depend on the holding time, hence the high relative abundance of manganese carbides in the 60-minute sample, similar to the study conducted by Bhalla and Eric (2015).

Observations made through the SEM-EDS analysis for the prereduced samples highlight the presence of textures different from those of the ore sample, with various phases representing the original minerals, reduced oxides, and increased silicate formation compared with the ore. All the identified phases host Mn in varied concentrations (refer to Table 6 for the abundances of the phases identified). The calcium manganese oxide is characterised by a porous texture, indicative of CO_2 loss from original carbonates, and consistent with reduction textures with rims of manganese oxide and carbides (Figures 3E and F). The phases that form part of the reduced material include manganese carbides, iron manganese, manganese magnesium oxide, and manganese oxides characterised

Table 6

Qualitative relative phase proportions in three prereduced samples investigating the effect of holding time concentration on reduction extent

Compound Name	Formula	20 Minutes	60 Minutes	90 Minutes
Manganosite	MnO	x	-	-
Iron manganese oxide	(Fe,Mn)O	xx	-	-
Manganese magnesium oxide	(Mg,Mn)O	xx	-	-
Manganese carbide A	Mn_7C_3	xx	xxxx	xxx
Manganese carbide B	Mn_5C_2	xx	xx	xx
Iron manganese	$Fe_{0.3}Mn_{0.7}$	x	xx	xx
Manganese iron carbide	$Mn_{1.8}Fe_{1.2}C$	xx	-	-
Graphite	C	xx	x	xx
Gehlenite	$Ca_2Al(AlSiO_7)$	xx	xx	xx
Bredigite	$Ca_7Mg(SiO_4)_4$	xx	xxx	xxx
Kirschsteinite	$CaFe^{2+}SiO_4$	xx	xx	xx
Calcium silicate	$Ca(SiO_3)$	xx	-	-

Not detected (-), trace (< 5% wt.% x), minor (5-15 wt.% xx), intermediate (15-30 wt.% xxx), major (30-50 wt.% xxxx) and predominant (>50 wt.% xxxxx)

by a high concentration of Mn and intergrown with silicate (Figures 3 C and D). Of all the materials identified, the silicate material is characterised by low Mn concentrations as opposed to the high Mn concentrations in the feed and reduced materials. The gehlenite and bredigite comprise the silicate materials occurring interstitially to the carbides, iron manganese, and manganese oxides (Figures 3C to F).

Overall, the samples display porous textures and smooth surfaces, representing the modification of structures and morphologies observed in the ore sample, similar to observations by Kononov (2008). In addition to the textural differences, the samples have variable oxide, alloy, and carbide coalescence, with the silicates representing the glass phase. The carbonates recorded in ore samples were completely decomposed by Reactions 9 and 10, since these phases were not observed in the prereduced products. The extent of the reduction in this study is determined by the presence of monoxides and carbides.

Lower Mn oxides versus manganese carbides

The carbides (Mn_7C_3, Mn_5C_2, and $(Fe_{1.8}Mn_{1.2})C$), oxides (MnO, FeO, $FeO_{0.198}(MnO)_{0.802}$, SiO_2, and MgO), and complex silicates ($Ca_3Mg(SiO_4)_2$, $Ca_2Al(AlSiO_7)$, $Ca_7Mg(SiO_4)_4$, and $CaFe^{2+}SiO_4$) identified in this study are quite similar to those typically found during the production of HCFeMn, MCFeMn, and LCFeMn, despite differences in carbon sources and operating conditions. Olsen et al. (2007) reported the HCFeMn producers typically produce alloy containing 78% Mn and 7% C, and slag containing around 40% MnO. The primary objective of HCFeMn/MCFeMn/LCFeMn is to create a manganese-rich alloy that enhances the strength, toughness, and wear resistance of steel. The carbon content in these alloys contributes to the mechanical properties of steel. Tangstad (2013) reported typical compositions of major commercial manganese alloys to have Mn ranging from 70 wt% to 82 wt% for HCFeMn, 75 wt% to 95 wt% for MCFeMn, and 85 wt% to 95 wt% for LCFeMn, with the corresponding C contents ranges being 6 wt% to 7.5 wt% , 1 wt% to 2 wt%, and 0.2 wt% to 0.5 wt%, respectively.

Producing carbides is more energy-efficient and cost-effective compared to producing pure manganese metal. The energy required to fully reduce MnO to metallic manganese without forming carbides is significantly higher (Coetsee, 2021), making it less economically viable for large-scale production. This is because the temperatures used in HCFeMn and MCFeMn production – around 1500 °C (Kononov et al., 2010) – favours the formation of carbides, with their Gibbs free energy being lower than that of metallic manganese (Kononov et al., 2009). Manganese's affinity for carbon and the reducing environment (high CO partial pressure) further stabilise carbides over oxides.

Conclusions

The study explored the mineralogical assessment of prereduced KMF Mamatwan-type manganese ore under different conditions using the CH_4-H_2-Ar gas mixture. The parameters investigated included understanding the effect of anthracite and methane concentration, as well as the effect of holding time on reduction extent. The mineralogical analysis highlights that the manganese ore was primarily reduced to manganese carbides, Mn_7C_3 and Mn_5C_2, which are preferred for the production of pure manganese metal. Other reduced phases included iron manganese and manganese oxide with their solid solution equivalents. Generally, the reduction using the CH_4-H_2-Ar gas mixture was effective and based on the results, the most desirable conditions for reduction are 8% anthracite, 10% methane, and 60 minutes of holding time, in agreement with the observations from the TGA tests. The overall results observed prove to be beneficial to the quest of lowering energy consumption and improving the overall efficiency of the smelting process.

Acknowledgements

The authors would like to thank Mintek for providing funding for this project.

References

Anacleto, N., Ostrovski, O., Ganguly, S. 2004. Reduction of manganese ores by methane-containing gas. *ISIJ international*, vol. 44, no. 10, pp. 1615–1622.

Bhalla, A., Eric, R.H. 2015. Reduction behavior of manganese ore using methane gas. In *The fourteenth international ferroalloys congress*, pp. 461–469.

Bhalla, A. 2018. *Hydrocarbon reduction of manganese ores*. University of the Witwatersrand (South Africa).

Chetty, D. 2008. *A geometallurgical evaluation of the ores of the northern Kalahari Manganese Deposit, South Africa*. University of Johannesburg (South Africa).

Chetty, D., Gutzmer, J. 2018. Quantitative mineralogy to address energy consumption in smelting of ores from the Kalahari Manganese Field, South Africa. *INFACON XV*, Cape Town, South Africa, pp. 25–28.

Coetsee, T. 2021. The Role of Metallic Iron in Low Temperature Carbothermic Reduction of MnO: Phase Chemistry and Thermodynamic Analysis. *Minerals*, vol. 11, no. 11, p. 1205.

Kononov, R. 2008. *Carbothermal solid state reduction of manganese oxide and ores in different gas atmospheres* (Doctoral dissertation, UNSW Sydney).

Kononov, R., Ostrovski, O., Ganguly, S. 2009. Carbothermal solid state reduction of manganese ores: 2. non-isothermal and isothermal reduction in different gas atmospheres. *ISIJ international*, vol. 687, no. 49, pp. 1107–1114.

Kononov, R., Ostrovski, O., Ganguly, S. 2010. June. Low temperature carbothermal reduction of siliceous manganese fines. In *Twelfth international ferroalloys congress sustainable future*, Helsinki, Finland, pp. 6–9.

Kuo, K., Persson, L.E. 1954. A contribution to the constitution of the ternary system Fe-Mn-C. *Isothermal sections at, 1050(910)*, pp.39–44.

Olsen, S.E., Olsen, S., Tangstad, M., Lindstad, T. 2007. *Production of manganese ferroalloys*. Tapir academic press.

Ostrovski, O., Anacleto, N., Ganguly, S. 2004. February. Reduction of manganese ores by methane containing gas. In *Proceedings Tenth International Ferroalloys Congress* (pp. 173–183).Rankin, W.J. and Van Deventer J.S.J. 1980. *Journal of the Southern African Institute of Mining and Metallurgy,* vol. 80, pp. 239–47.

Rankin, W.J., Wynnyckyj, J.R. 1997. Kinetics of reduction of MnO in powder mixtures with carbon. *Metallurgical and Materials Transactions B*, vol. 28, pp. 307–319.

Steenkamp, J.D., Bam, W.G., Ringdalen, E., Mushwana, M., Hockaday, S.A.C., Sithole, N.A. 2018. Working towards an increase in manganese ferroalloy production in South Africa-a research agenda. *Journal of the Southern African Institute of Mining and Metallurgy*, vol. 118, no. 6, pp. 645–654.

Tangstad, M. 2013. Manganese ferroalloys technology. In *Handbook of ferroalloys*, pp. 221–266. Butterworth-Heinemann.

Tangstad, M., Ichihara, K. and Ringdalen, E. 2015. Pretreatment unit in ferromanganese production. The *Fourteenth International Ferroalloys Congress. Energy efficiency and environmental friendliness are the future of the global ferroalloy industry*, Kiev, Ukraine, 31 May-4 June 2015, pp. 99–106.

U.S. Geological Survey. 2024. Mineral commodity summaries 2024: U.S. Geological Survey, 202 p., https://doi.org/10.3133/mcs2024

Wellbeloved, D.B., Craven, P.M., Waudby, J.W. 1990. Manganese and Manganese Alloys. In: Elvers, B., Hawkins, S. and Schulz, G. (Eds.) *Ullmann's Encyclopedia of Industrial Chemistry*. 5th Edition. vol. A16, pp. 77–121. ◆